0026-895X/97/020237-12$3.00/0

MOLECULAR PHARMACOLOGY, **52:**237–248 (1997).

Localization and Functional Expression of Splice Variants of the $P2X_2$ Receptor

JOSEPH SIMON, EMMA J. KIDD, FIONA M. SMITH, IAIN P. CHESSELL, RUTH MURRELL-LAGNADO, PATRICK P. A. HUMPHREY, and ERIC A. BARNARD

Molecular Neurobiology Unit, Royal Free Hospital School of Medicine, London, NW3 2PF, United Kingdom (J.S., E.A.B.), and Glaxo Institute of Applied Pharmacology (J.S., E.J.K., F.M.S., I.P.C., P.P.A.H.) and Department of Pharmacology (F.M.S., R.M.-L.), University of Cambridge, Cambridge CB2 1QJ, United Kingdom

Received December 26, 1996; Accepted April 24, 1997

SUMMARY

cDNAs encoding three splice variants of the $P2X_2$ receptor were isolated from rat cerebellum. The first variant has a serine/proline-rich segment deleted from the intracellularly located carboxyl-terminal domain of the $P2X_2$ subunit. The second and third variants have the splice site in the second half of the predicted first transmembrane domain. Either a 12-amino acid insertion or a six-amino acid deletion occurs at this position. cRNAs for these isoforms of the $P2X_2$ subunit were injected into *Xenopus laevis* oocytes and tested for function. ATP evoked inward currents only with the splice variant [designated $P2X_{2(b)}$] having the 69-amino acid deletion. The potencies of various agonists at the homomeric $P2X_{2(b)}$ receptor were not significantly different from those at the $P2X_{2(a)}$ homomeric channel. However, the $P2X_{2(b)}$ receptor showed significantly lower antagonist sensitivity. In contrast to the nondesensitizing $P2X_{2(a)}$ receptor, prolonged application of ATP produced a more rapid desensitization of the $P2X_{2(b)}$ receptor. When the $P2X_{2(a)}$ and $P2X_{2(b)}$ receptor responses were recorded in transfected mammalian cells, this difference was again found. The change in desensitization may be determined by proline/serine-rich segments and/or phosphorylation motifs that are removed from the tail region in formation of the $P2X_{2(b)}$ subunit. *In situ* hybridization of the three newly isolated isoforms of the $P2X_2$ subunit was performed at the macroscopic and cellular levels; transcripts for two of them [$P2X_{2(b)}$ and $p2x_{2(c)}$] but not the third [$p2x_{2(d)}$], which carries the 12-amino acid addition, were present in many structures in the neonatal rat brain and on sensory and sympathetic ganglia. mRNA for the $p2x_{2(d)}$ splice variant was present only in the nodose ganglion, at a low level.

Extracellular ATP has been established as a neurotransmitter in the central and peripheral nervous systems, producing its action via specific cell surface receptors, termed P2 receptors (1, 2). These receptors can be classified into two fundamentally distinct classes according to their functional and structural properties (3–5). The P2X receptors form a separate family within the general class of the transmitter-gated channels (5), whereas the P2Y receptors belong to the G protein-coupled receptor superfamily (3). ATP evokes fast excitatory responses through P2X channels in many types of peripheral and central neurons (4, 6, 7).

Recent cloning of cDNAs encoding P2X receptor subunits has revealed novel structural features. To date, seven subunits of P2X receptors have been isolated (8–18). These all have no primary sequence homology to other transmitter-gated channels, having only two deduced TMs. The amino and carboxyl termini are intracellular, separated by a large extracellular loop (4, 19). These subunits of the P2X receptors share 35–59% identity with each other. Each of them can form ATP-gated, cation-selective channels when expressed in *Xenopus laevis* oocytes or in mammalian cell lines (8–18). When they are expressed heterologously, they can be characterized by their differences in terms of agonist selectivity (especially sensitivity to α,β-meATP), rate of desensitization, and potency of the few presently known antagonists (4, 13, 17). However, these recombinant receptors, produced as homo-oligomeric channels, cannot always be correlated with the phenotypes observed in native tissues, suggesting that heteropolymerization of different P2X subunits may occur *in vivo* or that yet other P2X receptor subunits exist. Indeed, heteropolymerization of the recombinant $P2X_2$ and $P2X_3$ subunits has been shown to reproduce a naturally occurring phenotype (10). Transcripts for these recently isolated P2X receptors have been shown to be distributed in a subtype-specific manner throughout the rat central and peripheral nervous systems (17, 20).

ABBREVIATIONS: TM, transmembrane domain; α,β-meATP, α,β-methylene-ATP; 2-MeSATP, 2-methylthio-ATP; bp, base pair(s); HEPES, 4-(2-hydroxyethyl)-1-piperazineethanesulfonic acid; RT, reverse transcription; PCR, polymerase chain reaction; PPADS, pyridoxal phosphate-6-azophenyl-2′,4′-disulfonic acid; SSC, saline sodium citrate; NMDA, *N*-methyl-D-aspartate; EGTA, ethylene glycol bis(β-aminoethyl ether)-*N,N,N′,N′*-tetraacetic acid; HEK, human embryonic kidney.

In studying the brain $P2X_2$ receptor, we have discovered that alternative splicing of its precursor mRNA can occur, to produce three isoforms of the $P2X_2$ subunit. This raises the possibility that the heterogeneity of P2X receptors *in vivo* is greater than previously anticipated, and it might explain some of the differences in properties observed between native P2X receptors and the singly expressed recombinant forms. We have, therefore, examined whether the mRNAs for these additional forms are expressed in the rat brain and sensory and sympathetic ganglia, using *in situ* hybridization. We also describe the pharmacology of one of the splice variants, which was the only one of the three that could be functionally expressed both in *X. laevis* oocytes and in HEK 293 cells.

In keeping with the new International Union of Pharmacology receptor nomenclature guidelines (21), we have now designated the original recombinant $P2X_2$ receptor (9) as $P2X_{2(a)}$ and our new forms as $P2X_{2(b)}$, $p2x_{2(c)}$, and $p2x_{2(d)}$; the latter two must presently be written in lowercase letters (21) because their functional significance remains to be determined.

Experimental Procedures

Materials. Lipofectamine and all culture media and reagents were obtained from GIBCO-BRL (Paisley, UK). 2-MeSATP and PPADS were from RBI (Natick, MA). Suramin [8-(3-benzamido-4-methylbenzamido)naphthalene-1,3,5-trisulfonic acid] was a generous gift from Bayer. α,β-meATP, ATP, and all other chemicals were purchased from Sigma (Poole, UK).

RT-PCR. Total RNA was extracted from the cerebellum of neonatal (5-day-old) Sprague-Dawley rats, as described by Chomczynski and Sacchi (22). Poly(A)$^+$ RNA was purified on an oligo(dT)-cellulose column and treated with RNase-free DNase I (Stratagene, Cambridge, UK) for 30 min at 37°. First-strand cDNA was synthesized from 5 μg of poly(A)$^+$ RNA using an oligo(dT)$_{18}$ primer and Moloney murine leukemia virus reverse transcriptase (first-strand cDNA synthesis kit; Clontech, Palo Alto, CA). Control reactions in the absence of reverse transcriptase were also carried out. $P2X_2$ sequence-specific primers (45-mer each) used for RT-PCR were as described previously (20), as follows: forward primer 1, 5′-GCCCGGGGCTGCTGGTCCGCGTTCTGGGACTACGAGACGCCTAAC-3′ (amino terminus); reverse primer 1, 5′-CTTGAGGTAGTCACTCTTCTGGCTTGCAATGTTGCCCTTTGAGAA-3′ (extracellular loop); forward primer 2, 5′-TTCTCAAAGGGCAACATTGCAAGCCAGAAGAGTGACTACCTCAAG-3′ (extracellular loop); reverse primer 2, 5′-AAGTTGGGCCAAACCTTTGGGGTCCGTGGATGTGGAGTCCTGTTG-3′ (carboxyl terminus). RT-PCR was performed with 2 μl of the first-strand reaction using the forward and reverse primers (200 ng of each primer) in the presence of 200 μM levels of each deoxynucleoside triphosphate and 2.5 units of Dynazyme DNA polymerase (Flowgen, Sittingbourne, UK). The conditions were as follows: 94° for 1 min, 59° for 1 min, and 72° for 1 min for 40 cycles, with a final extension at 72° for 10 min. The resulting PCR products were cloned into the pCR II vector (TA cloning kit; Invitrogen, Leek, The Netherlands) according to the manufacturer's instructions and were sequenced using the Sequenase version 2.0 enzyme (Sequenase kit; Amersham, Little Chalfont, UK).

Generation of constructs containing the full coding regions of splice variants of the $P2X_2$ subunit. A cDNA containing the full coding region of the first splice variant of the $P2X_2$ receptor was generated by ligation into the $P2X_{2(a)}$ sequence of a partial cDNA (RC604), which carries a 207-bp deletion. Briefly, the plasmid containing RC604 was digested with *Cla*I and *Nde*I restriction enzymes (Boehringer Mannheim, Lewes, UK). The isolated 189-bp cDNA fragment carrying the splice site was then ligated together with the *Bam*HI-*Cla*I (1009-bp, 5′-end) and *Nde*I-*Not*I (540-bp, 3′-end) fragments of the $P2X_{2(a)}$ cDNA into the pCMV BK vector (Stratagene, Cambridge, UK), which had been predigested with *Bam*HI and *Not*I, to yield the $P2X_{2(b)}$ plasmid construct.

To obtain the full coding regions of the $P2X_2$ splice variants carrying an 18-bp deletion (RC202) or a 36-bp sequence insertion (RC201), the plasmids were digested with *Psp*AI (Stratagene, Cambridge, UK) and *Bst*EII (Boehringer Mannheim, Lewes, UK) restriction enzymes. Fragments containing the splice site for either variant (274 bp for RC202 or 328 bp for RC201) were then isolated and ligated into the $P2X_{2(a)}$ sequence cloned into the pcDNA I^{amp} vector (9), which had previously been digested with *Psp*AI and *Bst*EII, to yield $p2x_{2(c)}$ and $p2x_{2(d)}$ plasmid constructs. All constructs were then sequenced once more to confirm their identities.

***In vitro* transcription and oocyte expression.** Oocytes were obtained by ovariectomy from *X. laevis* frogs anaesthetized with 0.3% 3-aminobenzoic acid ethyl ester methane sulfonate. Mature oocytes (stages V/VI) were then defolliculated in calcium-free OR2 solution, containing 82.5 mM NaCl, 5 mM HEPES, 2.5 mM KCl, 1 mM $MgCl_2$, pH 7.6, and 3 mg/ml collagenase IA (Sigma), and were used on the same day for injection.

Capped cRNAs were transcribed *in vitro* from the $P2X_{2(a)}$ (9), $P2X_{2(b)}$, $p2x_{2(c)}$, and $p2x_{2(d)}$ plasmid constructs (all linearized with *Not*I) or from the $P2X_3$-pcDNA 3 plasmid (10) (linearized with *Xho*I). T3 RNA polymerase [for $P2X_{2(b)}$] or T7 RNA polymerase [for $P2X_{2(a)}$, $p2x_{2(c)}$, $p2x_{2(d)}$, and $P2X_3$] were used with the appropriate mMessage mMachine RNA transcription kit (Ambion, Austin, TX) to obtain cRNAs for these receptors. The cRNA synthesis was carried out according to the manufacturer's instructions. cRNAs (50–100 ng in 50 nl/oocyte) were microinjected into defolliculated oocytes from eight batches. The cells were maintained in ND96 medium, containing 96 mM NaCl, 5 mM HEPES, 2 mM KCl, 1.8 mM $CaCl_2$, 1 mM $MgCl_2$, pH 7.6, and 0.1 mg/ml gentamycin, at 18° for up to 7 days.

Two-electrode voltage-clamp recordings were made 2–6 days after the microinjections, using an OC-725C oocyte clamp amplifier (Warner Instrument Corp., Hamden, CT) and the Pulse software package, version 7.89 (HEKA Electronics, Lambracht, Germany). The microelectrodes were filled with 3 M KCl and had resistances of 0.5–2 MΩ. In all experiments the oocytes were clamped at a holding potential of −60 mV. The bath solution contained 100 mM NaCl, 2 mM HEPES, 1 mM $MgCl_2$, and 0.1 mM $BaCl_2$, pH 7.4, and was continuously perfused at a flow rate of 2 ml/min. All drugs were prepared in the bath solution and applied by pipette after the flow of the bath solution was stopped. Complete solution exchange in the bath chamber (~100 μl) was then achieved in <2 sec.

Cell culture and transient expression. HEK 293 cells were transiently transfected with the $P2X_{2(b)}$ plasmid construct using the lipofectamine method. Cells were plated onto poly-D-lysine-coated 13-mm coverslips (approximately 10,000 cells/coverslip) and transfected with 1 μg of plasmid DNA and 2 μl of lipofectamine per coverslip, in 0.25 ml of Dulbecco's modified Eagle medium. After incubation for 6 hr at 37° (8:92, v/v, CO_2/air atmosphere), the same volume of Dulbecco's modified Eagle medium containing 20% fetal calf serum was added. Coverslips were used for electrophysiological measurements 24 or 48 hr later. HEK 293 cells stably expressing the $P2X_{2(a)}$ receptor (23) were maintained using standard techniques (24) and plated onto coverslips when required.

Conventional tight-seal, whole-cell recordings (25) were made using an Axopatch 200B amplifier (Axon Instruments, Foster City, CA). Electrodes had resistances of 2–4 MΩ when filled with 145 mM cesium aspartate, 1 mM EGTA, 5 mM HEPES, 2 mM NaCl, 1 mM $MgCl_2$, 727 μM $CaCl_2$, pH 7.3 (osmolarity, 290 mosM). The extracellular solution consisted of 145 mM NaCl, 2 mM KCl, 1 mM $MgCl_2$, 2 mM $CaCl_2$, 10 mM HEPES, 10 mM D-glucose, pH 7.3 (osmolarity, 300 mosM). Currents were filtered with a corner frequency of 2–5 kHz (four-pole Bessel filter), digitized at 2–10 kHz, and stored on computer. Compensation (at least 80%) for series resistance (4–10 MΩ) was used. Only data from cells with a residual series resistance of <12 MΩ were analyzed. Cells were voltage-clamped at −70 mV.

Agonists were applied using a modified fast-flow (90-msec onset and 50-msec offset latency) U-tube system (24).

***In situ* hybridization.** Antisense oligonucleotide probes (42–45-mer) were designed to detect mRNAs specific to the $P2X_2$ receptor (20) and to the $P2X_2$ splice variants. A general probe for the $P2X_2$ receptor was directed against the 3′ end of the coding region (9) and was specific for this subunit, compared with the other P2X receptors, but it would hybridize with mRNAs for $P2X_{2(a)}$ and its splice variants [$P2X_{2(b)}$, $p2x_{2(c)}$, and $p2x_{2(d)}$] (5′-AAGTTGGGCCAAACCTTTGGGGTCCGTGGATGTGGAGTCCTGTTG-3′). Probes for each of the three splice variant mRNAs were designed for regions where the sequence divergence occurred, as follows: $P2X_{2(b)}$, 5′-ATGCTGGCCAAGTGTGTCCACCACCTTGTCGAACTTCTTATGGCT-3′ (overlapping the 207-bp deletion site in the intracellular carboxyl terminus); $p2x_{2(c)}$, 5′-CTCGCTGTCCTGGTAGCTTTTCACACGAAGTAAAGCAGGATGAG-3′ (overlapping the 18-bp deletion site in TM1); $p2x_{2(d)}$, 5′-TTTCTGCACGATGAAGACGTACCTGTGGGACAGGGCGGTGCC-3′ (overlapping the novel 36-bp sequence spliced into TM1).

In situ hybridization was carried out essentially as described previously (20). Briefly, the probes were 3′ end-labeled with [^{35}S]2′-deoxy-5-*O*-(1-thio)dATP (>1000 Ci/mmol; Amersham, Little Chalfont, UK), using terminal deoxynucleotidyl transferase (Promega, Southampton, UK), and were purified on a Sephadex G-50 column. Coronal sections (12-μm thick) of neonatal (5-day-old) Sprague-Dawley rat brain and sections (12-μm thick) of nodose, superior cervical, and dorsal root ganglia from adult animals were cut and thaw-mounted onto gelatin-coated slides. After fixation of the tissues, parallel sections were hybridized with the four different probes, overnight at 37°, in a moist chamber. The composition of the hybridization buffer was exactly as described earlier (20). Parallel control sections were hybridized in the presence of a 50-fold excess of the appropriate unlabeled probes.

After hybridization, the sections were rinsed with 1× SSC (15 mM sodium citrate, 150 mM NaCl, pH 7.0) (21°, 5 min), washed three times with 1× SSC (55°, 30 min), and finally washed with 1× SSC (21°, 60 min). The sections were then dehydrated, air-dried, and exposed to Hyperfilm βmax (Amersham) for 6 weeks. Both ganglia and brain sections were also dipped in Ilford K5 autoradiographic emulsion (Ilford, Knutsford, UK), exposed for 6 or 16 weeks, respectively, and counterstained with hematoxylin and eosin or methylene blue, respectively.

Statistical analysis. All values are expressed as the mean (of n determinations) ± standard error or, in the case of EC_{50} values, as the geometric mean (and 95% confidence interval). Differences in mean values were considered to be significant at $p < 0.05$, using an unpaired Student's t test.

Results

Amplification of partial cDNAs by RT-PCR. PCR performed on neonatal rat cerebellum first-strand cDNA with the first set of $P2X_{2(a)}$ receptor-specific primers (forward 1/reverse 1) always produced two products; one gave a broad band in the gel at ~620 bp and the other yielded a sharper band at ~660 bp (Fig. 1, *lane 2*). When the PCR amplification was repeated using the second primer set (forward 2/reverse 2), it also yielded two differently sized products (approximately 620 and 820 bp) (Fig. 1, *lane 5*). Subcloning and sequencing of these products revealed that two of the products (624 bp, amplified using the first set of primers, and 825 bp, amplified using the second set of primers) were identical in sequence to segments of the $P2X_{2(a)}$ cDNA previously isolated from the PC-12 pheochromocytoma cell line (9). However, three other partial cDNAs were also identified by sequencing of the subcloned products; they were either

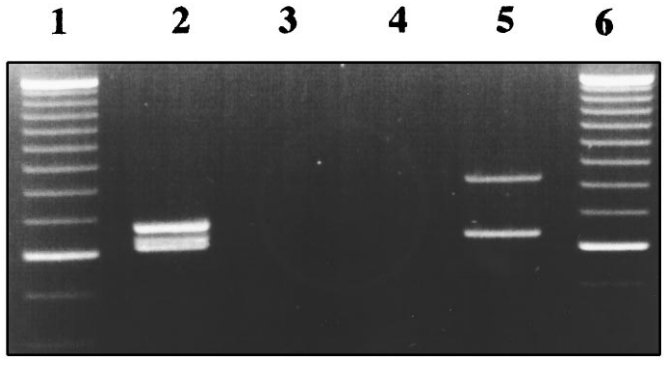

Fig. 1. Agarose gel electrophoresis of the cDNAs isolated by PCR. The gel (2%) was stained with ethidium bromide. *Lanes 1* and *6*, 100-bp DNA ladder (GIBCO/BRL). *Lane 2*, PCR amplification products obtained from neonatal rat cerebellum poly(A)$^+$ RNA with forward and reverse primers 1. The lower band corresponds to the predicted size (624 bp) of the $P2X_{2(a)}$ cDNA plus the 606 bp of the $p2x_{2(c)}$ partial cDNA; the upper band corresponds to the predicted size (660 bp) of the $p2x_{2(d)}$ cDNA. *Lanes 3* and *4*, control reactions performed either in the absence of template cDNA (*lane 3*) or without reverse transcriptase in the first-strand reaction (*lane 4*). *Lane 5*, products with forward and reverse primers 2; the upper band corresponds to the predicted size (825 bp) of the $P2X_{2(a)}$ cDNA and the lower band to the 618 bp of the $P2X_{2(b)}$ cDNA. The PCR amplifications with each of the primer sets were repeated at least six times from two different first-strand cDNA syntheses, using different cerebellar mRNA preparations.

smaller or larger than the predicted sizes for the corresponding $P2X_{2(a)}$ cDNA fragments. The first isolated partial cDNA (RC604) was found to be identical in sequence to the corresponding $P2X_{2(a)}$ fragment except that a 207-bp sequence was deleted. In this case the splicing occurred toward the carboxyl terminus, where a serine/proline-rich region (69 amino acids) was spliced out, starting at the Val-370 codon (Fig. 2C). The other two partial cDNAs differed in sequence from the corresponding $P2X_{2(a)}$ fragment in that one (RC201) had a 36-bp (12-amino acid) addition in the TM1 domain (at the Trp-46 codon) (Fig. 2B), whereas the second (RC202) had an 18-bp (six-amino acid) deletion at the same position (Fig. 2A). In both cases this TM was interrupted; however, the first few of the 12 amino acids spliced into this region in RC201 were hydrophobic enough to allow formation of a new TM (MVQLLILLYFVWVASGAGTAL) to be predicted.

Alignment of the partial cDNAs with the genomic DNA sequence for the rat $P2X_2$ subunit, which has been reported by Brändle *et al.* (26), revealed that the first intron is within TM1 and the 36-bp insertion into the TM1 domain (RC201) is entirely from translated intronic sequence at the 3′ end of this first intron (Fig. 2B). [Three bases in our sequence are absent from the reported (26) intronic sequence, without causing a frame shift (Fig. 2B); our sequence was confirmed by analysis of several clones obtained after PCR.] A cryptic splice site within the first intron was apparently used in the splicing process. The 18-bp deletion that occurs in the same position (RC202), however, represents the 5′ end of the following exon being spliced out with intron I, using another cryptic acceptor site in that exon (Fig. 2A). The 207-bp deletion that occurs in the third partial cDNA (RC604) creates another $P2X_2$ isoform having that deletion from the carboxyl-terminal exon. This alternative splice site is not flanked by introns (Fig. 2C), with two cryptic splice sites in the exon sequence being used. All of the splice sites used in forming the altered transcripts fit into the GT-AG rule (Fig. 2), even

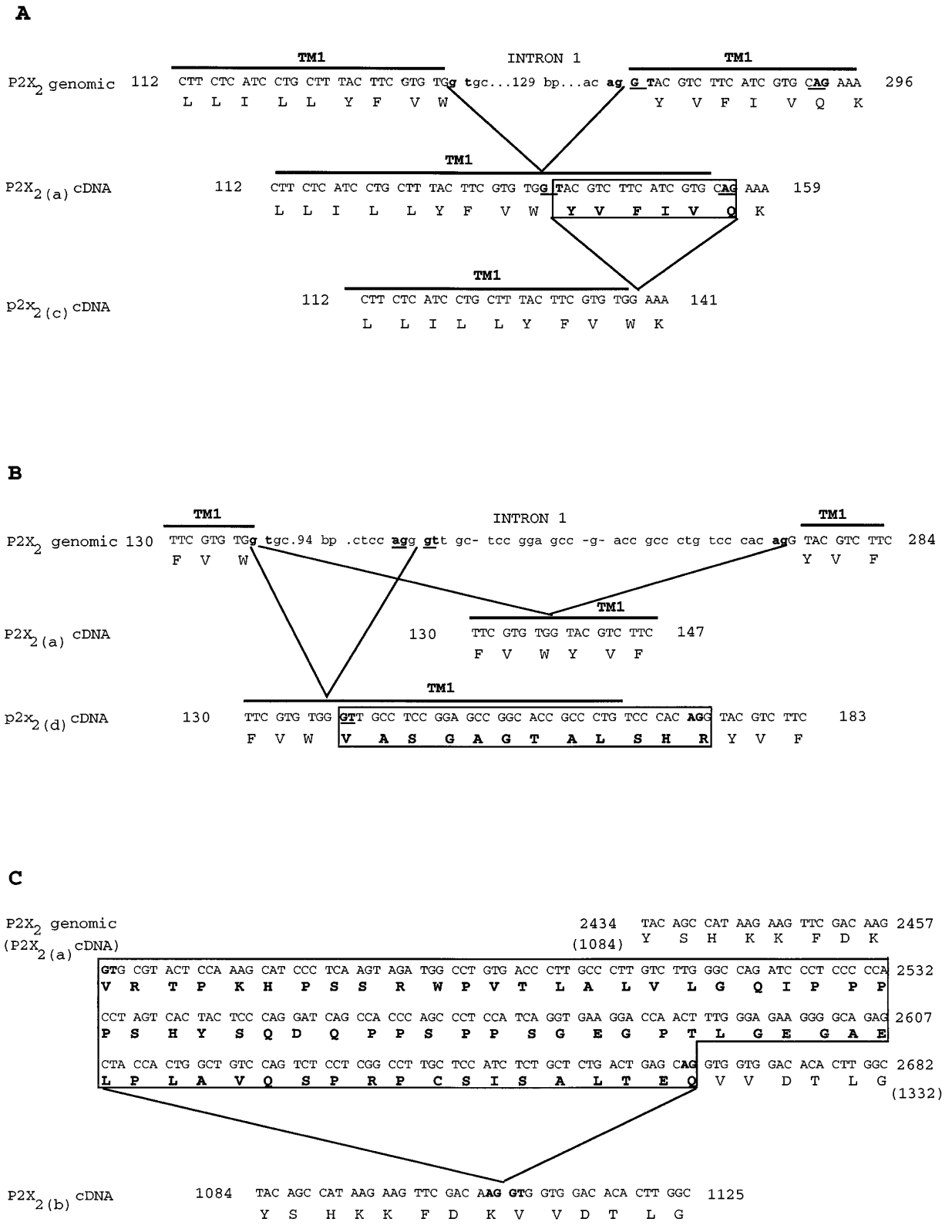

Fig. 2. Comparison of the cDNA sequences of $P2X_{2(b)}$, $p2x_{2(c)}$, and $p2x_{2(d)}$ with $P2X_{2(a)}$ and $P2X_2$ genomic DNA sequences. The figure shows only the parts of the DNA sequences, and the predicted amino acid sequences, where the alternative splicing occurs. Numbering of the DNA sequences starts at the beginning of the coding region (A of ATG). Base numbers for the $P2X_{2(a)}$ cDNA in C are shown in parentheses. The intronic sequences are in lowercase letters. The consensus bases for splice donor and acceptor sites are in *bold type*, and the cryptic site consensus bases are also *underlined*. The 69-amino acid deletion [$P2X_{2(b)}$] (C), the six-amino acid deletion [$p2x_{2(c)}$] (A), and the 12-amino acid addition [$p2x_{2(d)}$] (B) are *boxed* and in *bold type*. The genomic DNA sequence of the $P2X_2$ subunit is from the report of Brändle *et al.* (26) (EMBL accession number Y09910), and the $P2X_{2(a)}$ sequence is from the report of Brake *et al.* (9) (GenBank accession number U14414). The full DNA sequences of the splice variants of the $P2X_2$ subunit presented here have been deposited in the EMBL database [accession numbers Y10473 for $P2X_{2(b)}$, Y10474 for $p2x_{2(c)}$, and Y10475 for $p2x_{2(d)}$].

with the extended consensus sequences C/AAG|GTA/GAGT (for splice donor site) and $(T/C)_nNC/TAG|G$ (for splice acceptor site) (27).

Isolation of full-length cDNAs encoding splice variants of the $P2X_2$ subunit. It was confirmed, by PCR amplification using the $P2X_{2(a)}$ subunit-specific forward primer 1 in combination with the reverse primer 2, that the splice variants contained no additional splice sites. This primer set should amplify almost the whole coding region of each variant and would reveal any other splice sites if they existed. However, the PCR amplification yielded products of the predicted size for each variant, with only one splice site each (data not shown). Full-length cDNAs of the $P2X_2$ receptor splice variants [$P2X_{2(b)}$, $p2x_{2(c)}$, and $p2x_{2(d)}$] were constructed by inserting the appropriate partial cDNA fragments (RC604, RC202, and RC201), carrying the deletion or insertion, into the original $P2X_{2(a)}$ receptor DNA sequence (Fig. 2).

Expression of the splice variants of the $P2X_2$ receptor. Properties of the $P2X_{2(b)}$, $p2x_{2(c)}$, and $p2x_{2(d)}$ splice variants in comparison with the $P2X_{2(a)}$ receptor were investigated by expression in *X. laevis* oocytes. Oocytes microinjected with $p2x_{2(c)}$ and $p2x_{2(d)}$ cRNAs showed no response to a range of P2 receptor agonists (Fig. 3A). These included ATP (500 μM), 2-MeSATP (100 μM), α,β-meATP (500 μM), and ADP (1 mM). No inward currents were detectable when the experiments were repeated with different batches of oocytes injected with two different preparations of each of the cRNAs (data not shown). Parallel experiments, in which oocytes from the same batch were injected with $P2X_{2(a)}$ (9) or $P2X_3$ (10) cRNAs, always responded to ATP (Fig. 3A), suggesting that these two splice variants of the $P2X_{2(a)}$ receptor are not expressed or are not functional. No response to any agonist was found when the $p2x_{2(c)}$ or $p2x_{2(d)}$ cRNA-injected oocytes were voltage-clamped at different voltages (−80 mV to +60 mV). Additionally, $p2x_{2(c)}$ or $p2x_{2(d)}$ cRNAs were coinjected with $P2X_{2(a)}$ cRNAs; the properties of the $P2X_2$ channel measured then showed no difference from the properties (as in Fig. 3A) of the $P2X_{2(a)}$ homo-oligomeric channel (data not shown).

In contrast, when $P2X_{2(b)}$ cRNA was microinjected into *X. laevis* oocytes, ATP (300 μM) always evoked large inward currents, similar in size to those seen for the $P2X_{2(a)}$ receptor (Fig. 3A). Whereas the ATP-induced current in oocytes expressing the $P2X_{2(a)}$ receptor showed very little desensitization during prolonged application of ATP (300 μM), that mediated by the splice variant $P2X_{2(b)}$ receptor desensitized more rapidly (Fig. 3A). The decay phases of these responses mediated by $P2X_{2(a)}$ and $P2X_{2(b)}$ receptors were fitted with a single-exponential function, with time constants of 112.0 ± 10.7 sec (n = 5) and 27.5 ± 2.0 sec (n = 10), respectively. Responses to 30 μM ATP had decay time constants of 267 ± 30.9 sec (n = 10) and 45.9 ± 6.5 sec (n = 6) for $P2X_{2(a)}$ and $P2X_{2(b)}$, respectively. Although the rate of desensitization for the $P2X_{2(b)}$ receptor was fast, compared with that of $P2X_{2(a)}$, it was still relatively slow, compared with that of $P2X_3$ receptors expressed in oocytes from the same batch (Fig. 3A). Indeed, agonist-induced responses at the latter subtype have been shown to decay within ~10 msec (10, 11).

The concentration-effect relationships for ATP, 2-MeSATP, and α,β-meATP at the $P2X_{2(a)}$ and $P2X_{2(b)}$ receptors are shown in Fig. 3B. Current amplitudes were normalized to the peak amplitude of the response evoked by 300 μM ATP in each oocyte. The relationships for $P2X_{2(b)}$ were very similar to those for $P2X_{2(a)}$. ATP and 2-MeSATP were full agonists at both receptors; the EC_{50} values for ATP were 28 μM (95% confidence interval, 21–38 μM) [$P2X_{2(a)}$] and 18 μM (95% confidence interval, 11–28 μM) [$P2X_{2(b)}$], and those for 2-MeSATP were 25 μM (95% confidence interval, 14–46 μM) [$P2X_{2(a)}$] and 21 μM (95% confidence interval, 6–82 μM) [$P2X_{2(b)}$]. α,β-meATP evoked very small currents at both receptors, such that the maximum responses recorded were ≤15% of the response to 300 μM ATP.

The P2 receptor antagonists suramin and PPADS reduced the ATP-evoked currents in oocytes expressing either $P2X_{2(a)}$ or $P2X_{2(b)}$ receptors. The antagonism by both suramin and PPADS was significantly less at the $P2X_{2(b)}$ receptor than at the $P2X_{2(a)}$ receptor (Table 1).

The functional properties of the splice variant $P2X_{2(b)}$ receptor were also investigated in a mammalian expression system. HEK 293 cells were transiently transfected with the $P2X_{2(b)}$ plasmid construct, and the electrophysiological properties of the expressed receptor were compared with those of the $P2X_{2(a)}$ receptor stably expressed in HEK 293 cells. ATP (100 or 300 μM) evoked inward currents at the stably expressed $P2X_{2(a)}$ receptor in all cells tested (Fig. 4A), as reported previously (24). About 20% of all cells transiently transfected to express the $P2X_{2(b)}$ subunit responded to ATP, typical of the transfection efficiency under our conditions. In those responding cells, the induced current was similar in size to the currents evoked at stably expressed $P2X_{2(a)}$ receptors. This current, however, desensitized faster, as had been observed in the oocyte expression study (Figs. 3A and 4). Single-exponential decays could not be adequately fitted to all recordings, and the results are expressed as a percentage of the residual current remaining after a 10-sec application of ATP. The residual ATP-induced currents (at both 100 and 300 μM) were significantly smaller at the transiently expressed splice variant $P2X_{2(b)}$ receptor than at the $P2X_{2(a)}$ receptor (34.6 ± 4.7 versus 71.4 ± 3.8% at 100 μM and 41.1 ± 3.4 versus 63.8 ± 2.3% at 300 μM) (Fig. 4B).

***In situ* hybridization in the central nervous system.** In adult brain a very weak signal was seen for each of the splice variants of the $P2X_2$ subunit except for the $p2x_{2(d)}$ form, which was absent (data not shown). Therefore, the macroscopic distributions of the mRNAs for the newly isolated $P2X_2$ receptor splice variants $P2X_{2(b)}$, $p2x_{2(c)}$, and $p2x_{2(d)}$ were examined in parallel sections throughout the neonatal (5-day-old) rat brain. Representative autoradiograms are shown at the level of the dorsal hippocampus in Fig. 5. The specific labeling could be eliminated in the control sections by incubation with a 50-fold excess of the appropriate unlabeled oligonucleotide; an example is shown for the general $P2X_2$ receptor probe (Fig. 5D). The distribution of the signal for mRNAs for the $P2X_{2(b)}$ or $p2x_{2(c)}$ receptors was similar throughout the neonatal rat brain, with few apparent quantitative differences (Table 2). There was no detectable signal, however, for $p2x_{2(d)}$ transcripts in any area of the brain. The most intense labeling for all of the detectable transcripts was seen in the piriform layer of the cortex, with the signal being almost as intense in the CA1 to CA3 regions of the hippocampus, the dentate gyrus, and the ventromedial hypothalamus (Fig. 5).

The cellular localization of $P2X_{2(b)}$ transcripts in strongly labeled areas of the neonatal brain, such as the piriform

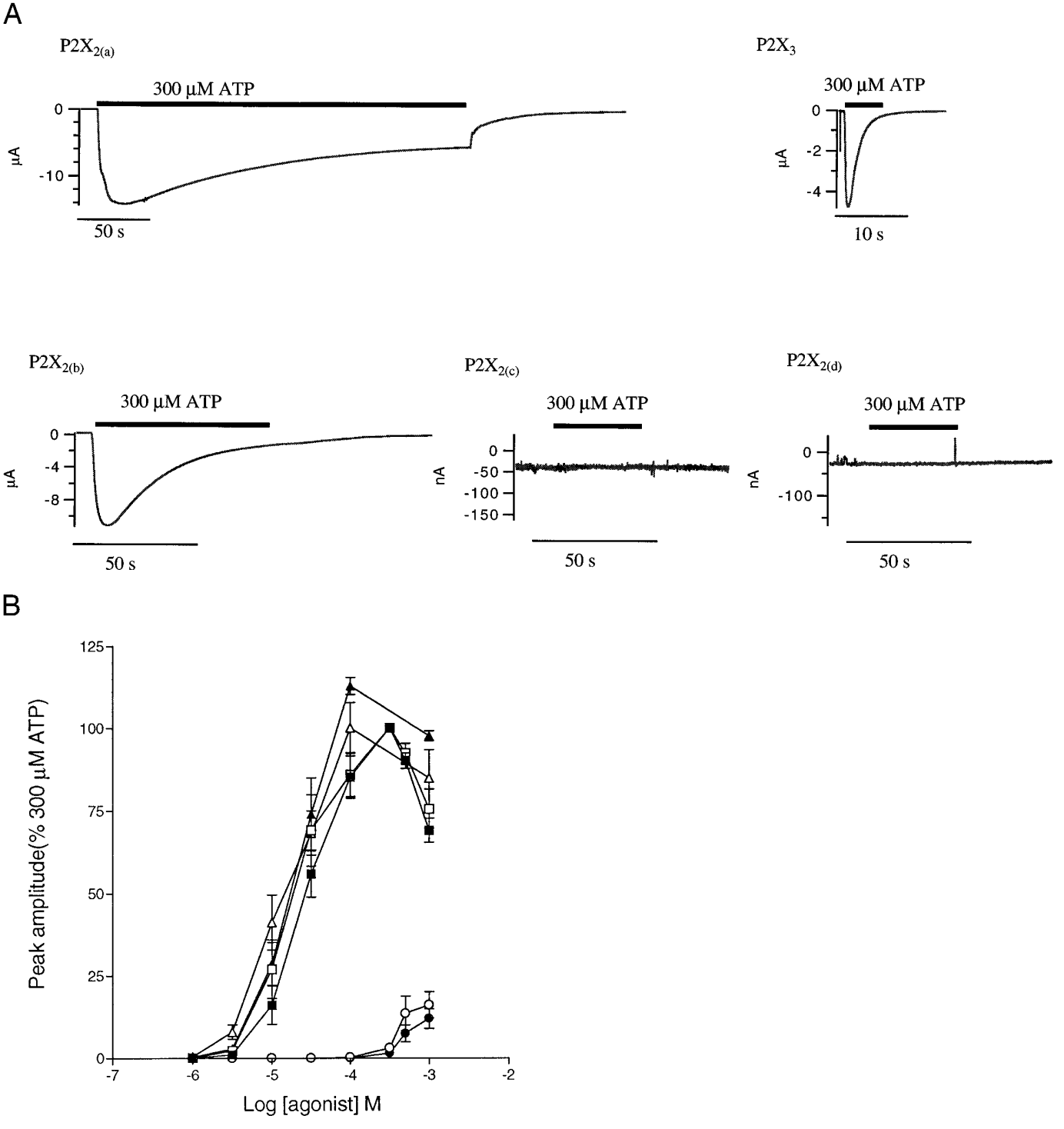

Fig. 3. Functional expression of the $P2X_{2(b)}$ splice variant in *X. laevis* oocytes. A, ATP-evoked inward currents in oocytes injected with the $P2X_{2(b)}$, $p2x_{2(c)}$, and $p2x_{2(d)}$ cRNAs, in comparison with the currents in oocytes expressing the $P2X_{2(a)}$ or $P2X_3$ subunits. Currents were recorded during prolonged application of 300 μM ATP (holding potential, −60 mV). Note that ATP evoked no current with $p2x_{2(c)}$ or $p2x_{2(d)}$ cRNA-injected oocytes. Traces are representative of the others obtained [n = 5 oocytes each for $P2X_{2(a)}$, $P2X_3$, $p2x_{2(c)}$, and $p2x_{2(d)}$; n = 10 for $P2X_{2(b)}$]. B, Concentration-effect relationships for ATP (*squares*), 2-MeSATP (*triangles*), and α,β-meATP (*circles*), with $P2X_{2(a)}$ (*filled symbols*) and $P2X_{2(b)}$ (*open symbols*). To account for the variability and time dependence of channel expression, the data from each oocyte were normalized with respect to the current amplitude evoked by 300 μM ATP in that oocyte. Note that significant desensitization occurs with application of high concentrations of agonist.

cortex, the CA3 region of the hippocampus, the supraoptic nucleus, the ventromedial hypothalamic nucleus, and the cerebellum, is shown in Fig. 6 (see also Table 2). Intense labeling was seen in the pyramidal cells of the piriform cortex (Fig. 6A) and the CA1 to CA3 regions of the hippocampus (Fig. 6C; Table 2); a strong signal was also seen in the granule cell layer of the dentate gyrus (Table 2). Cell bodies in several hypothalamic nuclei, including the supraoptic, dorsomedial, and, in particular, ventromedial nuclei also exhibited strong signals (Fig. 6, E and G; Table 2); lower levels of

TABLE 1

Effects of P2 receptor antagonists on ATP-induced oocyte currents at the $P2X_{2(a)}$ receptor and its splice variant $P2X_{2(b)}$ expressed in *Xenopus* oocytes

Data are expressed as the percentage of the ATP-induced current that remained after continuous application of the antagonist or the vehicle (which was the buffer used externally).

	Current			
	$P2X_{2(a)}$		$P2X_{2(b)}$	
	30 μM ATP	300 μM ATP	30 μM ATP	300 μM ATP
	%			
Vehicle	95.6 ± 3.8 (n=3)[a]	98.3 ± 10.3 (n= 3)	105.6 ± 11 (n=3)	97.0 ± 3.5 (n=3)
Suramin (30 μM)	2.2 ± 0.9 (n= 5)	19.3 ± 1.0 (n= 5)	3.0 ± 0.5 (n=5)	39.3 ± 1.7[b] (n=5)
PPADS (3 μM)	3.8 ± 0.9 (n= 6)	7.9 ± 1.0 (n=10)	6.4 ± 1.4 (n=6)	13.5 ± 2.1[b] (n=7)

[a] n, number of oocytes used for the recordings.
[b] Statistically different from the equivalent value for the $P2X_{2(a)}$ receptor.

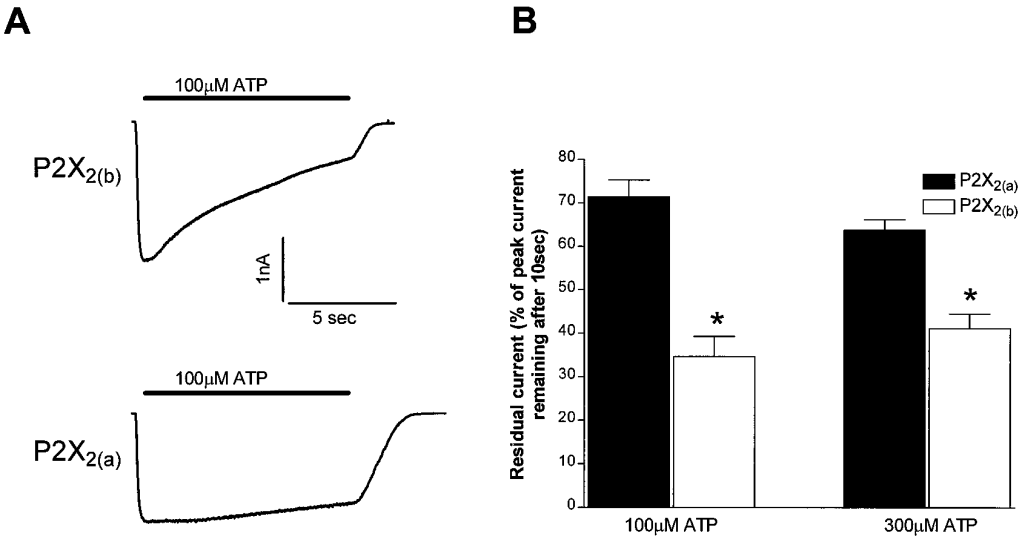

Fig. 4. Functional expression of the $P2X_{2(a)}$ and $P2X_{2(b)}$ receptors in HEK 293 cells. Responses were recorded either from cells stably expressing the $P2X_{2(a)}$ receptor (24) or from cells transiently expressing the $P2X_{2(b)}$ receptor (holding potential, −70 mV). A, Representative traces of the ATP-evoked inward current at the $P2X_{2(a)}$ and $P2X_{2(b)}$ receptors. B, Desensitization of ATP-induced currents at the $P2X_{2(a)}$ and $P2X_{2(b)}$ receptors. Residual currents are expressed as percentages of the peak current (at 100 or 300 μM ATP) remaining after a 10-sec application. *Bars,* mean determinations from at least 10 cells [*, significant difference from $P2X_{2(a)}$ current].

signal were detected in other cortical regions such as the cingulate and retrosplenial cortex (Table 2). Low levels of transcripts were found in the mitral cells of the olfactory tubercle and in cell bodies in the striatum and medial habenula (Table 2). In the hindbrain the cell bodies of the locus ceruleus were labeled by the probes specific for each splice variant and also by the oligonucleotide for the $P2X_2$ receptor. $P2X_{2(b)}$ and $p2x_{2(c)}$ transcripts were also evident in the cell bodies of the mesencephalic trigeminal nucleus and the spinal trigeminal nucleus and in its tract (Table 2). In the cerebellum both the Purkinje cell and granule cell layers were labeled, with a more intense signal being seen in the Purkinje cells (Fig. 6I; Table 2).

***In situ* hybridization in the peripheral nervous system.** The distributions of mRNA for the three splice variants described here were examined in two sensory ganglia (nodose and dorsal root) and in one sympathetic ganglion (superior cervical) at the cellular level. The results are summarized in Table 2. The most intense signal was seen in the cell bodies of the nodose ganglion for all types of $P2X_2$ mRNA, although the signal for the $p2x_{2(d)}$ transcript was weaker than those seen for the other two splice variants. The labeling of the $p2x_{2(c)}$ receptor transcript in the nodose ganglion was seen to be concentrated over the neuronal cell bodies, whereas the surrounding satellite cells remained unlabeled (Fig. 7A). This was also seen for the other splice variants (data not shown). mRNAs for the $P2X_{2(b)}$ and $p2x_{2(c)}$ splice variants were also detected in the cell bodies of the superior cervical ganglion. However, mRNA for $p2x_{2(d)}$ was barely detectable in this ganglion (Table 2). The lowest levels of mRNAs were found in the cell bodies of the dorsal root ganglia for all $P2X_2$ subunit-specific probes, and the signal for $p2x_{2(d)}$ transcripts was just detectable there (Table 2). The labeling for $p2x_{2(c)}$ mRNA appeared to be concentrated in a subpopulation of cells in the dorsal root ganglion, whereas the other mRNAs showed more widespread localization (data not shown).

Discussion

Splicing. We have isolated cDNAs encoding three splice variants of the original $P2X_2$ subunit (9). At least one of these, the $P2X_{2(b)}$ subunit, was functional when expressed in either *X. laevis* oocytes or mammalian HEK 293 cells. Two distantly separated splicing sites are apparently present to form these variants. One involves a significant shortening of the carboxyl-terminal region by 69 amino acids, with 207 bp spliced out directly from the interior of the carboxyl-terminal exon (26) (Fig. 2C). The other generates two alternative isoforms in TM1. In one isoform a 18-bp fragment is spliced out from exon II together with the whole of intron I, using a cryptic splice site located at the 5′ end of that exon (Fig. 2A). A similar situation has been described for the γ-aminobutyric

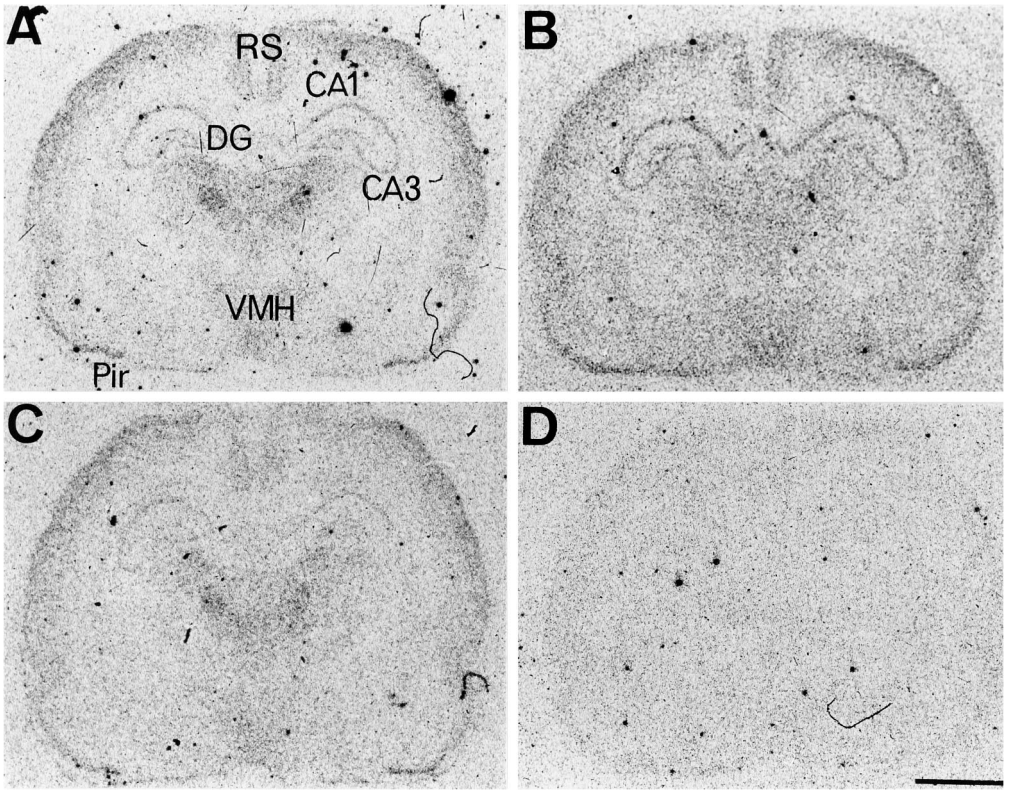

Fig. 5. Autoradiograms of coronal sections from a neonatal (5-day-old) rat brain at the level of the dorsal hippocampus. The parallel sections were hybridized with ^{35}S-labeled oligonucleotides specific for the $P2X_2$ (A), $P2X_{2(b)}$ (B), and $p2x_{2(c)}$ (C) receptor cDNAs. The representative control section (D) was hybridized in the presence of a 50-fold excess of the unlabeled general $P2X_2$ probe. Exposure time was 6 weeks. *CA1* and *CA3*, fields CA1 and CA3 of the hippocampus, respectively; *DG*, dentate gyrus; *Pir*, piriform cortex; *RS*, retrosplenial cortex; *VMH*, ventromedial hypothalamic nucleus. *Scale bar*, 2 mm.

acid$_A$ receptor β4 subunit, where two alternatively spliced variants arise by the use of one of two 5′ donor sites, which are separated by only 12 bp (28). In the second variant a 36-bp fragment insertion occurs at the same position. Although this segment is part of intron I, it is uninterrupted and in-frame with the following exonic sequence (Fig. 2B). In this case the alternative splicing uses another cryptic splice site located within that intron. Use of cryptic acceptor sites within an intron and translation of intronic sequences has also been found elsewhere, e.g., in the neurexin IIIα gene; use of one or another cryptic site within the intron located at the carboxyl-terminal region generates a large number of alternatively spliced isoforms (29).

TABLE 2

Distribution of transcripts for the splice variants of the $P2X_2$ subunit in the rat central and peripheral nervous systems

Signals were scored as absent (−), just detectable (±), low (+), moderate (++), strong (+++), or intense (++++)

Brain region	$P2X_2$	$P2X_{2(b)}$	$p2x_{2(c)}$	$p2x_{2(d)}$
Olfactory bulb	+	++	+	−
Cingulate cortex	++	+	+	−
Striatum	+	+	+	−
Retrosplenial cortex	++	+++	++++	−
Piriform cortex	++++	+++	++++	−
Hippocampus				
CA1 field	+++	+++	+++	−
CA2 field	+++	+++	++	−
CA3 field	+++	+++	++	−
Dentate gyrus	+++	+++	+++	−
Medial habenula	+	+	+	−
Dorsomedial hypothalamus	++++	++	++	−
Ventromedial hypothalamus	++++	+++	+++	−
Supraoptic nucleus	+++	++	++	−
Locus ceruleus	++++	++	+	−
Mesencephalic trigeminal nucleus	+++	++	+	−
Spinal trigeminal nucleus	++	++	+	−
Spinal trigeminal tract	+	+	+	−
Cerebellum	+++	++	++	−
Ganglia				
Nodose	++++	+++	++++	+
Superior cervical	+++	++	++	±
Dorsal root	+	+	+	±

With respect to the splice site in the TM1 domain, one can regard the $p2x_{2(c)}$ form as the parent form, with splicing in of either an 18-bp exon or that exon plus another (36-bp) exon. An equivalent situation, of a single- or double-short exon incorporation at one site, is found in another transmitter-gated channel subunit, the NR1 subunit of NMDA receptors, and leads to pharmacological differences for each of the forms thus generated (30). In the present case, it was shown by full-length sequencing that insertion at the first site is not linked to a change at the second, carboxyl-terminal, splicing site. Hence, no sequences were detected in which a change from the $P2X_{2(a)}$ structure occurred at both of these potential splice sites.

Alternative splicing of pre-mRNA is a common mechanism in the case of other transmitter-gated channels, whereby there is an increase in the number of subunit sequences available for channel assembly. Such splicing variants had not previously been characterized for the P2X receptor series. The only previous possible indication was the recent description (31) of a $P2X_2$-related cDNA clone with an inserted 85-bp sequence starting in the TM2 coding region, but this would be expected to terminate translation about two thirds of the distance down TM2. This was isolated as a partial cDNA, and no functional expression of such a truncated form has been reported. This 85-bp insertion can now be seen to be identical to intron X of the $P2X_2$ genomic sequence (26), i.e., it represents an incompletely processed mRNA.

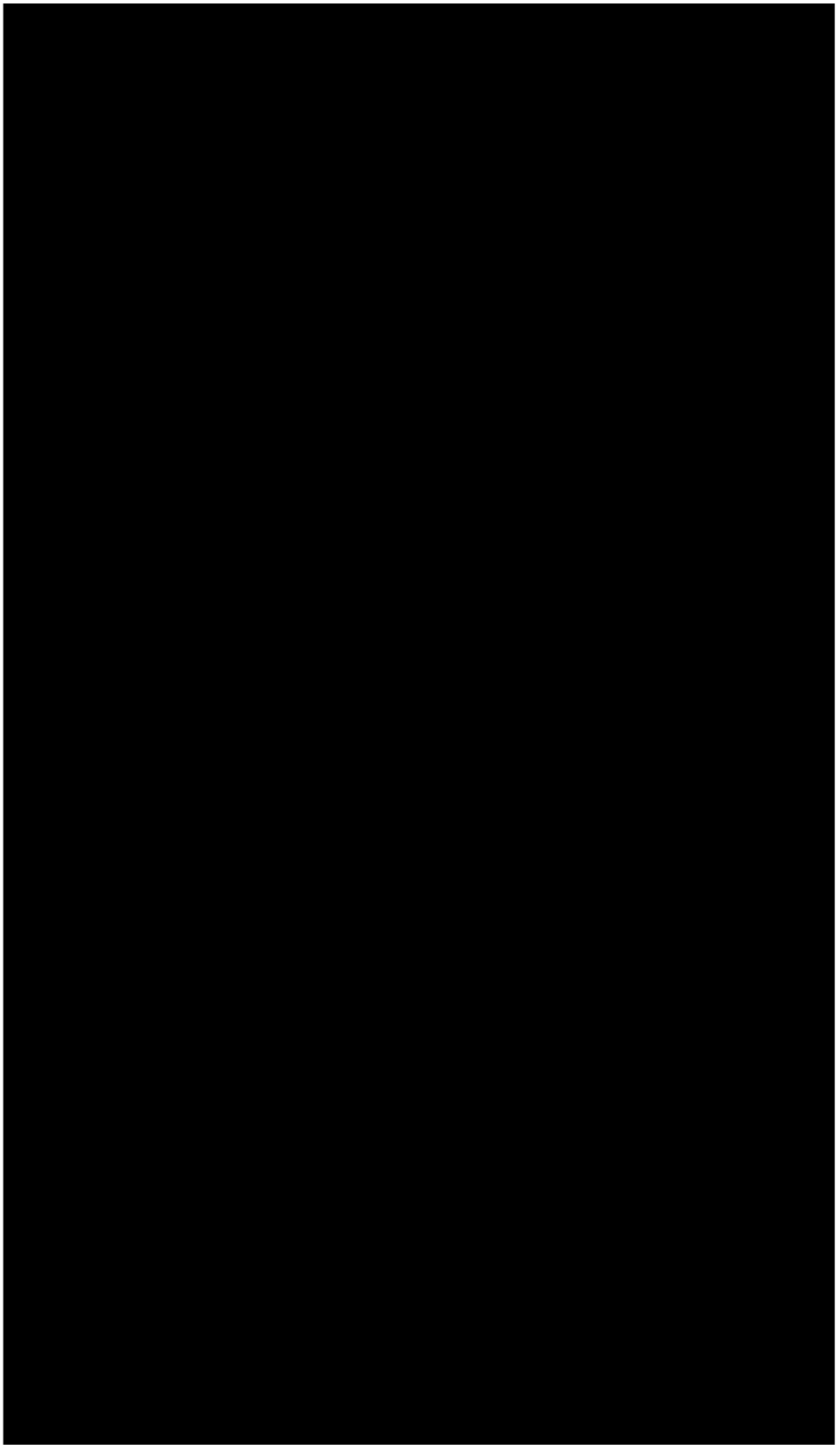

Fig. 6. Emulsion photomicrographs (original magnification, ×400) of methylene blue-stained sections of neonatal (5-day-old) rat brain. Exposure time was 16 weeks. A, C, E, G, and I, Cellular localization of the $P2X_{2(b)}$ transcript in the piriform cortex (A), the CA3 field of the hippocampus (C), the supraoptic nucleus (E), the ventromedial hypothalamic nucleus (G), and the cerebellum (I). B, D, F, H, and J, Corresponding controls hybridized in the presence of a 50-fold excess of the unlabeled probe. *EGL*, external granule cell layer; *MoCb*, molecular layer of cerebellum; *Pk*, Purkinje cell layer.

$P2X_{2(b)}$ receptor isoform. This form is of particular interest because we have shown it to be functional (Fig. 3). It has a 69-amino acid (207-bp) deletion starting at the Val-370 codon. A serine- and proline-rich region is thus deleted, shortening the carboxyl-terminal region (which is presumed to be intracellular in all P2X subunits) (19). This serine/proline-rich region is not found in any other known P2X receptor subtype. It contains at least three recognition se-

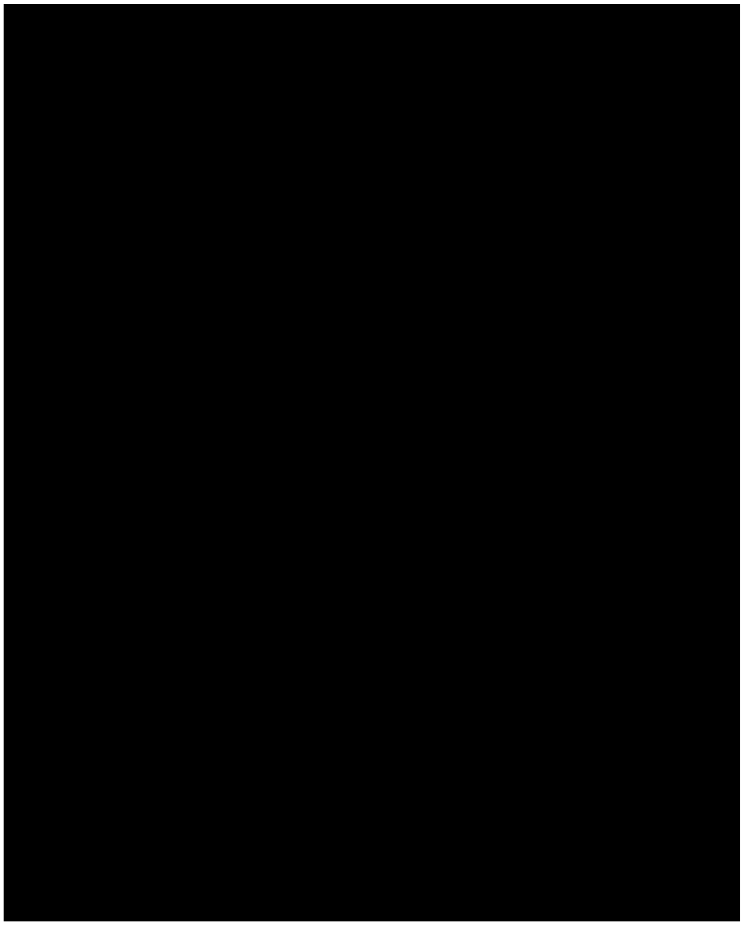

Fig. 7. Emulsion photomicrographs (original magnification, ×400) of hematoxylin/eosin-stained sections of adult rat nodose ganglia, showing mRNAs for the $p2x_{2(c)}$ splice variant. Exposure time was 6 weeks. A, mRNA for $p2x_{2(c)}$ located in the cell bodies. B, Corresponding control section hybridized in the presence of a 50-fold excess of the unlabeled probe.

quence motifs for serine kinases, i.e., KXXSX for myosin-I heavy-chain kinase, XSPX for proline-dependent protein kinase, and XSRX for cGMP-dependent protein kinase (32) (where X is any amino acid). It has been established for other transmitter-gated channels that receptor phosphorylation plays an important role in the regulation of various channel functions such as desensitization, subunit assembly, and receptor clustering (33, 34). Furthermore, this region contains two short hydrophobic segments highly enriched in prolines (ALVLGQIPPPP and PPSPP), very similar to those found in the epithelial sodium channel αrENaC, in the NMDA receptor 2D subunit, and in some other transmembrane proteins such as the Na^+/H^+ antiporter, the rat muscle Cl^- channel ClC-I, and the $Na^+/K^+/2Cl^-$ co-transporter (35). This domain is found (as here) at or near the carboxyl terminus of these proteins and is thought to be involved in the formation of complexes through association with the SH3 domain of certain intracellular signaling and cytoskeletal proteins, such as Src-like tyrosine kinases (36), Grb2 adapter protein and SOS nucleotide exchange factor (37), as well as α-spectrin (35). The SH3 type of interaction may, therefore, play a regulatory role for the $P2X_{2(a)}$ subunit in intracellular signaling or protein clustering at the plasma membrane. It may target $P2X_{2(a)}$ receptors to a location on the neuronal surface that is different from that of the $P2X_{2(b)}$ receptors. Neither $P2X_{2(a)}$ nor any other of the known P2X receptor subunits possesses the alternative carboxyl-terminal motif, present in some glutamate receptor subunits (38), for interaction at the PDZ binding sites of postsynaptic density proteins involved in the assembly of multiprotein complexes at the plasma membrane.

The $P2X_{2(b)}$ subunit presumably forms a homo-oligomeric channel when it is expressed in *X. laevis* oocytes, where it always produced a large ATP-induced inward current (Fig. 3A). The parameters of this current and the agonist selectivity profile of the $P2X_{2(b)}$ receptor were very similar to those of the $P2X_{2(a)}$ form, as found here and as previously observed for the latter (9, 24). ATP and 2-MeSATP were full agonists in both, with very similar EC_{50} values for the two receptor subtypes, whereas α,β-meATP had very little effect at either receptor (Fig. 3B). The two receptors showed a slightly different antagonist sensitivity, i.e., to suramin and PPADS, which was statistically significant (Table 1). However, whereas the channel formed by the $P2X_{2(a)}$ subunit either in *X. laevis* oocytes or in HEK 293 cells showed very little or no desensitization during prolonged application of an agonist (as also found previously) (9, 24), in both systems the $P2X_{2(b)}$ channel desensitized more rapidly (Figs. 3A and 4). Its rate of desensitization was, nevertheless, still much slower than that observed with the fast desensitizing P2X subunits such as $P2X_1$ (8, 24) and $P2X_3$ (Fig. 3A) (10, 11). The introduction in the $P2X_{2(a)}$ subunit of a serine/proline-rich carboxyl-terminal region, discussed above, is the most likely reason for this change in receptor desensitization. It was recently shown by North (19), from domain-exchange experiments between $P2X_1$ and $P2X_2$ subunits, that both TM1 and TM2 are needed for the very fast desensitization phenotype but the extracellular domain between them does not affect this.

However, we must now infer that an additional stage of control of desensitization can be exerted when the carboxyl-terminal chain is modified by alternative splicing.

Other known transmitter-gated ion channel subunits have (as here) a number of phosphorylation sites for cAMP dependent-protein kinase A, protein kinase C, or tyrosine kinase in an intracellular domain (33). Phosphorylation of these channels modulates the desensitization process (33, 34). Also, it is not known how the two proline-rich domains also present in the spliced sequence here affect the desensitization rate. Whatever the carboxyl-terminal sites involved, they exert a finer control of that rate than the all-or-none effect resulting from the TM1 and TM2 sequences. An additional possible interpretation is that the channels formed using $P2X_{2(b)}$ subunits are less tightly anchored to certain cytoskeletal or membrane proteins than $P2X_{2(a)}$ channels, because of the decrease in interactive domains (discussed above) in the new carboxyl terminus. This would influence conformational changes in the receptor; therefore, this is another possible mechanism for an intermediate rate of desensitization. These potential roles of the carboxyl-terminal motifs under consideration could be probed in future studies of mutagenesis and domain exchange focused on these sequences.

$p2x_{2(c)}$ and $p2x_{2(d)}$ receptor isoforms. Two of the $P2X_2$ cDNAs [$p2x_{2(c)}$ and $p2x_{2(d)}$] isolated in this study showed that splicing occurred at the Trp-46 codon, i.e., in the second half of the predicted TM1 (Fig. 2). The change, relative to the previously known $P2X_{2(a)}$ subunit sequence, gives either the addition of a 12-amino acid sequence [$p2x_{2(d)}$] or the deletion of six amino acids [$p2x_{2(c)}$]. In both cases the predicted TM1 for the $P2X_2$ is interrupted. In the first case, the alternative splicing occurs at a spare acceptor site (cryptic site) located in intron I (Fig. 2B). Because the 3′ end of that intron is not interrupted by a stop codon and it is in-frame with the following exon (Fig. 2B), this intronic sequence can be successfully translated. The first few residues of this segment inserted thus into the $P2X_{2(a)}$ receptor sequence are hydrophobic enough to allow formation of a novel TM to be predicted (Fig. 2B). Because the extracellular loop, which appears to contribute to the ATP binding site (19), is not changed, a functional subunit might be expected. On the other hand, for the deletion that occurs at the Trp-46 site [$p2x_{2(c)}$] and is attributed to the alternative use of a cryptic acceptor site in the 5′ region of the second exon (Fig. 2A), the question of whether the remaining TM1 sequence of only 16 amino acids can traverse the plasma membrane must be raised. If it does not, it would leave this isoform of the $P2X_2$ receptor anchored to the plasma membrane through only one hydrophobic domain (the original TM2), with the amino-terminal domain now presumed to be extracellular. However, because the remaining 16-residue stretch of TM1 is immediately preceded by an adjacent glycine, and because 17-residue TMs have been deduced to exist in several cases for other ion channels/receptors (e.g., Ref. 39), it is not certain that such a loss of TM1 would occur. In fact, the mRNA of this variant, $p2x_{2(c)}$, is almost as well expressed in the brain as the functional variants (Table 2). Translation of each of the transcripts can actually occur, because poly(A)$^+$ RNA transcribed from each of the splice variant cDNAs [$P2X_{2(a)}$, $P2X_{2(b)}$, $p2x_{2(c)}$, and $p2x_{2(d)}$] was shown in the reticulocyte *in vitro* translation (nonmicrosomal) system (Promega) to yield protein products to similar extents, with the predicted sizes.[1] The main difference seen between the $p2x_{2(c)}$ and $p2x_{2(d)}$ isoforms, therefore, was that the $p2x_{2(d)}$ mRNA was not expressed at detectable levels in the brain (neonatal or adult). The $p2x_{2(d)}$ form was, however, expressed in the nodose ganglion (Table 2), albeit at a lower level then the other forms there. This may indicate a specific role for it in some cells of such ganglia.

The absence of any functional responses to nucleotides of the expressed $p2x_{2(c)}$ subunit, although its mRNA is well expressed in many brain regions, is somewhat surprising and could be the result of one of several possible causes. It may be that the deletion in it leads to a differently folded protein that becomes trapped *en route* to the cell membrane in the oocyte system but this does not occur in its native neuronal environment because specific chaperones or targeting factors are present there. Alternatively, it [but not $P2X_{2(a)}$ or $P2X_{(b)}$] might require a partner subunit to form an active channel. These possibilities can be tested experimentally in future studies. Again, because TM1 and TM2 and adjacent residues appear, from domain-switch evidence (19), to seriously affect channel function, it may be that the shortening of TM1 perturbs the channel structure too much for functionality.

mRNAs for $P2X_{2(b)}$ and $p2x_{2(c)}$ subunits have the same distribution pattern throughout the rat central (neonatal) and peripheral (adult) nervous systems, with minor quantitative differences in some brain regions such as the olfactory bulb, CA2 and CA3 fields of the hippocampus, locus ceruleus, mesencephalic trigeminal nucleus, and spinal trigeminal nucleus, where the $P2X_{2(b)}$ transcript is apparently expressed at higher levels (Table 2). Because we examined the transcript distribution at the neonatal stage, for greater overall mRNA abundance, it is possible that these isoforms are expressed more specifically or exclusively in certain locations at various developmental stages. This phenomenon is known for splice variants of other transmitter-gated channel subunits; for example, some isoforms of the NR1 subunit of the NMDA receptor (30) are expressed differentially at different developmental stages. mRNAs for some of the NR1 isoforms are not detectable until postnatal day 7 or 8, whereas others have peaked in their expression by then, with their level decreasing in certain brain areas to the adult age. Determination of possible differences in localization and levels of the mRNAs for the splice variants of the $P2X_2$ subunits throughout the central and peripheral nervous systems of rats at different developmental stages is therefore now warranted. Likewise, the present conclusions on the distribution of the isoforms are limited here by the nonavailability of suitable antibodies specific for each; measurement of the abundance of the four $P2X_2$ receptor proteins on cell membranes in each brain region is required for additional approaches ascertaining their functional significance.

Finally, after this article was submitted for publication, a report on the genomic organization of the $P2X_2$ subunit was kindly sent to us by Brändle *et al.* (26). Those authors found a splice variant that is identical in both structural and functional properties to our $P2X_{2(b)}$ isoform.

[1] F. M. Smith, unpublished observations.

Acknowledgments

We thank Drs. G. Buell for kindly providing the rat $P2X_{2(a)}$ and $P2X_3$ clones, A. Surprenant for the HEK 293 cell line stably expressing the rat $P2X_{2(a)}$ receptor, and T. E. Webb and A. D. Michel for helpful advice during the course of this work.

References

1. Fredholm, B. B., M. P. Abbracchio, G. Burnstock, J. W. Daly, T. K. Harden, K. A. Jacobson, P. Leff, and M. Williams. VI. Nomenclature and classification of purinoceptors. *Pharmacol. Rev.* **46:**143–156 (1994).
2. Zimmermann, H. Signalling via ATP in the nervous system. *Trends Neurosci.* **17:**420–426 (1994).
3. Barnard, E. A., G. Burnstock, and T. E. Webb. G protein-coupled receptors for ATP and other nucleotides: a new receptor family. *Trends Pharmacol. Sci.* **15:**67–71 (1994).
4. Surprenant, A., G. N. Buell, and R. A. North. P_{2X} receptors bring new structure to ligand-gated ion channels. *Trends Neurosci.* **18:**224–229 (1995).
5. Barnard, E. A. The transmitter-gated channels: a range of receptor types and structures. *Trends Pharmacol. Sci.* **17:**305–309 (1996).
6. Edwards, F. A., and A. J. Gibb. ATP: a fast neurotransmitter. *FEBS Lett.* **325:**86–89 (1993).
7. Galligan, J. J., and P. P. Bertrand. ATP mediates fast synaptic potentials in enteric neurons. *J. Neurosci.* **14:**7563–7571 (1994).
8. Valera, S., N. Hussy, R. J. Evans, N. Adami, R. A. North, A. Surprenant, and G. N. Buell. A new class of ligand-gated ion channel defined by P_{2X} receptor for extracellular ATP. *Nature (Lond.)* **371:**516–519 (1994).
9. Brake, A. J., M. J. Wagenbach, and D. Julius. New structural motif for ligand-gated ion channels defined by an ionotropic ATP receptor. *Nature (Lond.)* **371:**519–523 (1994).
10. Lewis, C., S. Neidhart, C. Holy, R. A. North, G. N. Buell, and A. Surprenant. Heteropolymerization of P2X receptor subunits can account for ATP-gated currents in sensory neurons. *Nature (Lond.)* **377:**432–435 (1995).
11. Chen, C. C., A. N. Akopian, L. Sivilotti, D. Colquhoun, G. Burnstock, and J. N. Wood. A P2X purinoceptor expressed by a subset of sensory neurones. *Nature (Lond.)* **377:**428–430 (1995).
12. Bo, X., Y. Zhang, M. Nassar, G. Burnstock, and R. Schoepfer. A P2X purinoceptor cDNA conferring a novel pharmacological profile. *FEBS Lett.* **375:**129–133 (1995).
13. Buell, G. N., C. Lewis, G. Collo, R. A. North, and A. Surprenant. An antagonist-insensitive P_{2X} receptor expressed in epithelia and brain. *EMBO J.* **15:**55–62 (1996).
14. Séguéla, P., A. Haghighi, J.-J. Soghomonian, and E. Cooper. A novel neuronal P_{2X} ATP receptor ion channel with widespread distribution in the brain. *J. Neurosci.* **16:**448–455 (1996).
15. Soto, F., M. Garcia-Guzman, J. M. Gomez-Hernandez, M. Hollmann, C. Karschin, and W. Stuhmer. P2Xα4: an ATP-activated ionotropic receptor cloned from rat brain. *Proc. Natl. Acad. Sci. USA* **93:**3684–3688 (1996).
16. Wang, C., N. Namba, T. Gonoi, N. Inagaki, and S. Seino. Cloning and pharmacological characterization of a fourth P2X receptor subtype widely expressed in brain and peripheral tissue. *Biochem. Biophys. Res. Commun.* **220:**196–202 (1996).
17. Collo, G., R. A. North, E. Kawashima, E. Merlo-Pich, S. Neidhart, A. Surprenant, and G. N. Buell. Cloning of $P2X_5$ and $P2X_6$ receptors and the distribution and properties of an extended family of ATP-gated ion channels. *J. Neurosci.* **16:**2495–2507 (1996).
18. Surprenant, A., F. Rassendren, E. Kawashima, R. A. North, and G. N. Buell. The cytolytic P2Z receptor for extracellular ATP identified as a P2X receptor (P2X7). *Science (Washington D. C.)* **272:**735–738 (1996).
19. North, R. A. P2X purinoceptor plethora. *Semin. Neurosci.* **8:**187–197 (1996).
20. Kidd, E. J., C. B. A. Grahames, J. Simon, A. D. Michel, E. A. Barnard, and P. P. A. Humphrey. Localization of P_{2X} purinoceptor transcripts in the rat nervous system. *Mol. Pharmacol.* **48:**569–573 (1995).
21. Vanhoutte, P. M., P. P. A. Humphrey, and M. Spedding. International Union of Pharmacology recommendations for nomenclature of new receptor subtypes. *Pharmacol. Rev.* **48:**1–2 (1996).
22. Chomczynski, P., and N. Sacchi. Single step method of RNA isolation by acid guanidinium thiocyanate-phenol-chloroform. *Anal. Biochem.* **162:**156–159 (1987).
23. Vulchanova, L., U. Arvidsson, M. Riedl, J. Wang, G. Buell, A. Surprenant, R. A. North, and R. Elde. Differential distribution of two ATP-gated ion channels (P_{2X} receptors) determined by immunocytochemistry. *Proc. Natl. Acad. Sci. USA* **93:**8063–8067 (1996).
24. Evans, R. J., C. Lewis, G. N. Buell, S. Valera, R. A. North, and A. Surprenant. Pharmacological characterization of heterologously expressed ATP-gated cation channels (P_{2x}-purinoceptors). *Mol. Pharmacol.* **48:**178–183 (1995).
25. Hamill, O. P., A. Marty, E. Neher, B. Sakmann, and F. J. Sigworth. Improved patch-clamp techniques for high resolution recording from cells and cell-free membranes. *Pflügers Arch.* **391:**85–100 (1981).
26. Brändle, U., P. Spielmanns, R. Osteroth, J. Sim, A. Surprenant, G. Buell, J. P. Ruppersberg, P. K. Plinkert, H.-P. Zenner, and E. Glowatzki. Desensitization of the $P2X_2$ receptor controlled by alternative splicing. *FEBS Lett.* **404:** 294–298 (1997).
27. Smith, C. W. J., J. G. Patton, and B. Nadal-Ginard. Alternative splicing in the control of gene expression. *Annu. Rev. Genet.* **23:**527–577 (1989).
28. Lasham, A., E. Vreugdenhil, A. N. Bateson, E. A. Barnard, and M. G. Darlison. Conserved organization of γ-aminobutyric $acid_A$ receptor genes: cloning and analysis of the chicken β4-subunit gene. *J. Neurochem.* **57:**352–355 (1991).
29. Ushkaryov, Y. A., and T. C. Südhof. Neurexin IIIα: extensive alternative splicing generates membrane-bound and soluble forms. *Proc. Natl. Acad. Sci. USA* **90:**6410–6414 (1993).
30. Zukin, R. S., and M. L. V. Bennett. Alternatively spliced isoforms of the NMDAR1 receptor subunit. *Trend Neurosci.* **18:**306–313 (1995).
31. Housley, G. D., D. Greenwood, T. Bennett, and A. F. Ryan. Identification of a short form of the P2xR1-purinoceptor subunit produced by alternative splicing in the pituitary and cochlea. *Biochem. Biophys. Res. Commun.* **212:**501–508 (1995).
32. Kemp, B. E., and R. B. Pearson. Protein kinase recognition sequence motifs. *Trends Biochem. Sci.* **15:**342–346 (1990).
33. Huganir, R. L., and P. Greengard. Regulation of neurotransmitter receptor desensitization by protein phosphorylation. *Neuron* **5:**555–567 (1990).
34. Swope, S. L., S. J. Moss, C. D. Blackstone, and R. L. Huganir. Phosphorylation of ligand-gated ion channels: a possible mode of synaptic plasticity. *FASEB J.* **6:**2514–2523 (1992).
35. Rotin, D., D. Bar-Sagi, H. O'Brodovich, J. Merilainen, V. P. Lehto, C. M. Canessa, B. C. Rossier, and G. P. Downey. An SH3 binding region in the epithelial Na^+ channel (αrENaC) mediates its localization at the apical membrane. *EMBO J.* **13:**4440–4450 (1994).
36. Koch, C. A., D. Anderson, M. F. Moran, C. Ellis, and T. Pawson. SH2 and SH3 domains: elements that control interactions of cytoplasmic signaling proteins. *Science (Washington D. C.)* **252:**668–674 (1991).
37. Buday, L., and J. Downward. Epidermal growth factor regulates $p21^{ras}$ through the formation of a complex of receptor, Grb2 adapter protein, and SOS nucleotide exchange factor. *Cell* **73:**611–620 (1993).
38. Kornau, H. C., L. T. Schenker, M. B. Kennedy, and P. H. Seeburg. Domain interaction between NMDA receptor subunits and the postsynaptic density protein PSD-95. *Science (Washington D. C.)* **269:**1737–1740 (1995).
39. Yamamoto-Hino, M., T. Sugiyama, K. Hikochi, M. G. Mattei, K. Hasegawa, S. Sekine, K. Sakurada, A. Miyawaki, T. Furuichi, M. Hasegawa, and K. Mikoshiba. Cloning and characterization of human type 2 and type 3 inositol 1,4,5-triphosphate receptors. *Recept. Channels* **2:**9–22 (1994).

Send reprint requests to: P. P. A. Humphrey, Glaxo Institute of Applied Pharmacology, Department of Pharmacology, University of Cambridge, Tennis Court Road, Cambridge CB2 1QJ, UK. E-mail: ppah0562@ggr.co.uk